Design and optimization of a nanoprobe comprising amphiphilic chitosan colloids and Au-nanorods: Sensitive detection of human serum albumin in simulated urine

Ren-Der Jean[a‡], Mikael Larsson[b‡], Wei-Da Cheng[c], Yu-Yuan Hsu[c], Jong-Shing Bow[d] and Dean-Mo Liu[c*]

[a]Material and Chemical Research Laboratories, Industrial Technology Research Institute, Hsinchu, Taiwan, ROC

[b]Future Industries Institute, University of South Australia, Mawson Lakes Campus, SA 5095, Australia

[c]Department of Materials Science and Engineering, National Chiao Tung University, Hsinchu, Taiwan, ROC

[d]Integrated Service Technology Inc., No. 19, Pu-ding Rd., Hsinchu, Taiwan

*Corresponding author:

deanmo.liu@gmail.com

Nano-Bioengineering Lab, Dept. Materials Science & Engineering

National Chiao Tung University

1001 Ta-Hseuh Road, Hsinchu, Taiwan

‡The authors contributed equally to this work.

Abstract

Metallic nanoparticles have been utilized as analytical tools to detect a wide range of organic analytes. In most reports, gold (Au)-based nanosensors have been modified with ligands to introduce selectivity towards a specific target molecule. However, in a recent study a new concept was presented where bare Au-nanorods on self-assembled carboxymethyl-hexanoyl chitosan (CHC) nanocarriers achieved sensitive and selective detection of human serum albumin (HSA) after manipulation of the solution pH. Here this concept was further advanced through optimization of the ratio between Au-nanorods and CHC nanocarriers to create a nanotechnology-based sensor (termed CHC-AuNR nanoprobe) with an outstanding lower detection limit (LDL) for HSA. The CHC-AuNR nanoprobe was evaluated in simulated urine solution and a LDL as low as 1.5 pM was achieved at an estimated AuNR/CHC ratio of 2. Elemental mapping and protein adsorption kinetics over three orders of magnitude in HSA concentration confirmed accumulation of HSA on the nanorods and revealed the adsorption to be completed within 15 minutes for all investigated concentrations. The results suggest that the CHC-AuNR nanoprobe has potential to be utilized for cost-effective detection of analytes in complex liquids.

Keywords: Surface plasmon resonance biosensor; Chitosan nanoparticles; Gold nanorods; Human serum albumin; Simulated urine

1. Introduction

Nanosized objects of noble metals, i.e., Au, Ag, Pd, etc., have received enormous interest as their physicochemical properties differs significantly from larger objects of these elements. In particular, surface plasmon resonance (SPR) has been investigated and used in a number of biomedical applications, including diagnostic sensing [1-6], bio-imaging [7-10] and therapeutic cancer therapy [11-13]. Development of cost-effective, readily available and reliable diagnostic biosensor technologies is especially important for the healthcare sector as early-stage detection of diseases offers both cost savings and dramatically improved clinical outcomes. To be an effective tool in such early stage diagnostics, biosensors must be capable of detecting very low concentrations of analyte, while also being highly selective in their response. Therefore, development of biosensors with improved performance depends on designs that are highly selective for interactions with the target analyte and that present a large number of detection sites and/or present a strong reporter signal upon a detection event. Nano-dimensional objects have been heavily investigated to this end as they present a huge surface area for analyte binding and as binding events commonly can be detected by readily available UV-visible or fluorescent spectroscopy.

Among the nano-dimensional objects used to construct biosensors, gold nanoparticles (AuNPs) have likely received the most attention. They present unique optoelectronic behavior, high surface-to-volume ratio and a chemistry that allows for modification with functional ligands for sensitive and selective responses to a target analyte. Such responses include changes in plasmonic resonance absorption, conductivity or emission spectrum in response to changes in the surrounding environment [14-18]. Despite their attractive properties, implementation of metal NPs (including AuNPs) in applications has been limited by that they are prone to

aggregation that weakens or eliminates their desirable properties. To prepare metal nanoparticles for realistic applications there has been much work on new synthetic strategies and surface modifications [19-22]. While the colloidal stability of AuNPs is critical to maintain their surface plasmon properties, it is equally important for biosensing applications that the biorecognition capability and response to the analyte is maintained [23]. Unfortunately, stabilizing molecules such as surfactants or other type of organic molecules on the AuNP surface often affect the SPR and may decrease the detection sensitivity.

There are, however, other routes than core-shell designs that result in excellent stability and biosensing performance of AuNPs. In a recent investigation we adsorbed bare-surface Au-nanorods (AuNR) onto positively charged nanocarriers of self-assembled amphiphilic carboxymethyl-hexanoyl chitosan (CHC) and investigated the system for detection of the protein *human serum albumin* (HSA) using conventional UV-visible spectroscopy [24]. The negatively charged AuNRs were rapidly adsorbed on the positively charged surface of the CHC nanocarriers and were thus stabilized as individual rods, forming a stable CHC-AuNR nanosuspension (termed "CHC-AuNR nanoprobe" in the forthcoming discussion). Importantly and interestingly, by manipulating the pH the electrostatic interactions between the CHC nanocarriers, HSA, and deposited Au-nanorods could be tuned for excellent sensitivity and selectivity towards the analyte, without the use of any targeting ligands. Although promising, a number of physiological challenges remain before this technology can be put to use and design parameters will need to be investigated and optimized for individual analytes and physiological environments.

In this work the CHC-AuNR nanoprobe was evaluated for detection of HSA in simulated urine (SU) while simultaneously investigating how the performance of the

system correlated with AuNR/CHC nanocarrier ratio and how the HSA adsorption kinetics depended on protein concentration. The selected model system is of relevance as the SU presents a moderately challenging environment that could interfere with the performance of the CHC-AuNR nanoprobe system and as the concentration of HSA in urine can be used as a marker for kidney function.

2. Methods

2.1. Materials

Gold nanorods with an aspect ratio of 5.2 were purchased from Nanorods, LLC, United States. Buffer solution (pH 5) was purchased from Alfa Aesar. Carboxymethyl-hexanoyl chitosan (CHC) was purchased from Advanced Delivery Technology Co, Taiwan. Ethanol (99.8%), creatine, Na_3PO_4, urea and albumin from human serum (HSA) were purchased from Sigma Aldrich and used as received. NaCl and KCl were purchased from J.T. Baker. All the solutions were prepared with ultrapure deionized water (DI water).

2.2. Preparation of simulated urine solution

To prepare SU 1.21 g of urea was added to 50 ml of DI water. Subsequently, 0.5 g NaCl, 0.3 g KCl, 0.32 g Na_3PO_4 and 0.133 g of creatine were added to the solution. Finally, different amounts of HSA were dissolved to achieve desired concentrations.

2.3. Preparation of CHC-AuNR nanoprobe solutions

CHC-AuNR nanoprobe solutions with different CHC to AuNR ratios were prepared by mixing 0.6, 0.45 or 0.3 ml AuNR solution ($2 \cdot 10^{11}$ AuNR/ml) with DI water to a final volume of 1 ml. Subsequently, the samples were centrifuged at 15000

rpm for 15 minutes before addition of 0.1 mL of 1 wt% CHC solution and mixing. Thereafter, 0.9 mL of ethanol was mixed with the dispersion to remove the CTAB from the AuNRs' surfaces. Finally, the samples were centrifuged at 15000 rpm for 30 minutes, the supernatant containing ethanol and CTAB was decanted and the gel-like CHC-AuNR-NPs were re-dispersed into 1 ml of DI water. The different volumes of added AuNR dispersion resulted in different AuNR/CHC nanocarrier ratios that were estimated as previously reported [24] to 4, 3, and 2, for added AuNR dispersion volumes of 0.6, 0.45 and 0.3 ml, respectively. Before use in analyte detection 0.5 ml of the CHC-AuNR dispersion was mixed with 0.5 ml of pH 5 buffer solution for pH control, effectively forming the completed CHC-AuNR nanoprobe solution.

2.4. Analyses

20 µl of the analyte solution was added drop-wise to 1 ml of the CHC-AuNR nanoprobe solution, followed by 15 minutes of incubation. Subsequently, absorption spectra were obtained using a UV-visible spectrophotometer (Thermo Scientific Evolution 3000, USA) and a quartz cuvette that had been cleaned by soaking in aqua regia and washed with DI water and ethanol. From the acquired spectra the peak shift was recorded for different HSA concentrations. Every test condition was measured three times on different samples and results are reported as averages with standard deviation, where applicable.

TEM and EDS mapping was performed using a JEOL JEM-2800F operated at 200 kV.

3. Results and discussion

3.1. Performance in simulated urine

It is known from the literature that both the absorbance maximum [25] and spectral shift in response to surrounding refractive index [26, 27] increases with the aspect ratio of an AuNR. In sensing applications, the increase in spectral shift with increasing aspect ratio is used for improved resolution and lower detection limit (LDL) when determining the analyte concentration. In this work, AuNRs with an average aspect ratio of 5.2 were utilized. See Table 1 for size characteristics and Fig. 1 for TEM image.

Table 1. Size characteristics of the gold nanorods. Each data point was obtained from at least 30 particles.

Length/nm	Diameter/nm	Aspect ratio
39±6.7	7±1.0	5.2±0.7

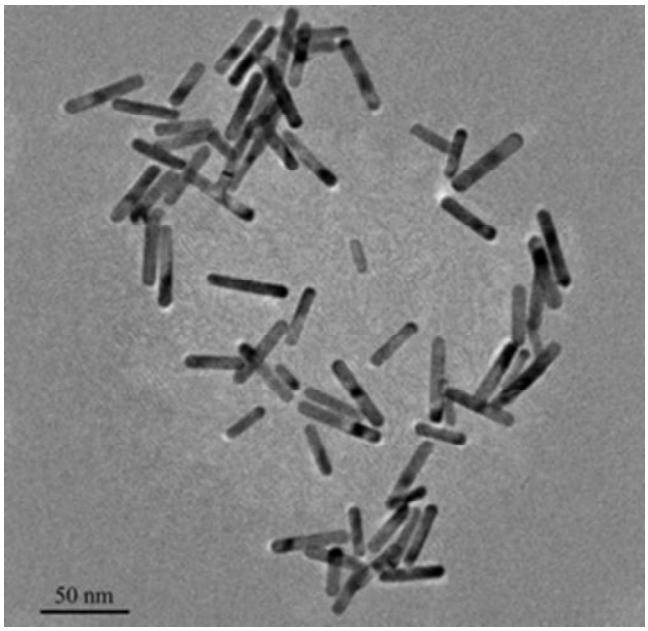

Fig. 1. TEM image of used AuNRs

In our previous work it was demonstrated that bare AuNRs could be assembled

onto CHC nanocarriers by simple mixing and removal of the CTAB by washing with ethanol, forming the CHC-AuNR nanoprobe system. The nanocarriers stabilized the AuNRs in solution with maintained sensitivity to the analyte. In contrast, CTAB stabilized nanorods presented poor sensitivity towards the analyte. It was further shown for the CHC-AuNR nanoprobe in DI water that the adsorption of HSA and lysozyme on the Au-NRs was highly selective and effective close to the isoelectric point (IEP), pH = 5 and pH = 9 for HSA and lysozyme, respectively [24]. This behavior was explained by pH dependent electrostatic interactions that caused the analytes to preferentially adsorb on the AuNR-surfaces close to the IEP. The implications are that the nanoprobe system can be tuned towards selective detection of analytes through optimization of solution pH, i.e., the selectivity is not dependent on any specific ligands.

In this work the CHC-AuNR nanoprobe was evaluated and optimized for detection of HSA in SU. As a first step the absorption spectrum of the CHC-AuNR nanoprobe was recorded in DI water and SU and was compared with that of AuNRs. As shown in Fig. 2a the CHC-AuNR nanoprobe presented a peak value that was red-shifted about 5 nm compared to pure AuNRs. However, there was little difference in peak values (about 0.1 nm) between DI water and SU at pH = 5. The similar peak values suggested that there was little-to-no interference from the compounds in the SU (i.e., creatine and urea) for the CHC-AuNR nanoprobe configuration used in the subsequent analyses (prepared with pH 5 buffer). The difference in absorbance may be due to slight differences in concentration or physicochemical factors, such as aggregation. However, since the peak shift is the critical parameter for the sensing, no further attention was given to the slight difference in absorbance. The peak shift in response to HSA concentration was also investigated in SU or DI water for the

CHC-AuNR system with an AuNR/CHC ratio of 4. As seen in Fig. 2b the peak shift response was well resolved in the concentration range 10^5 – 10^8 fM. At higher concentrations the response plateaued, likely due to saturation of the available NR surface, and the variability between measurements increased.

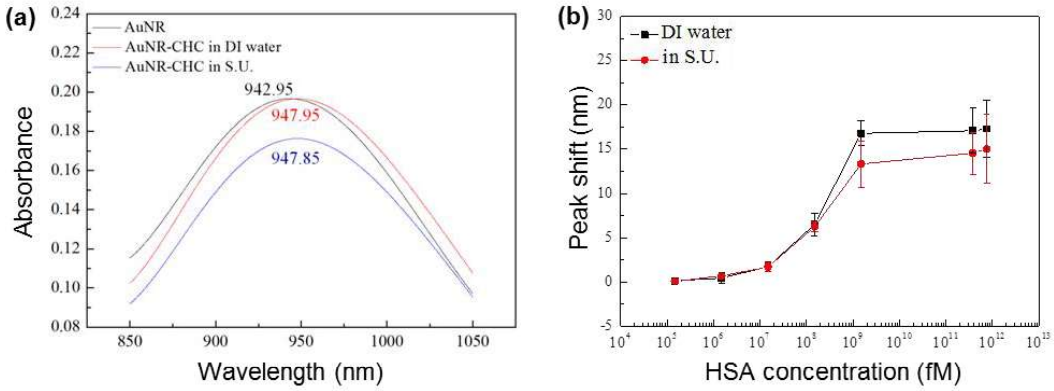

Fig. 2. (a) UV-visible spectra at pH 5 in DI water and SU solution for CHC-AuNR nanoprobe and AuNRs. (b) Peak shift for the nanoprobe system with AuNR/CHC ratio of 4 in response to different HSA concentrations in SU or DI water.

3.2. The effect of AuNR/CHC ratio on lower detection limit

The LDL of SPR-based sensors for various applications has been a subject of interests over the last decade [28-31]. Here the impact of the ratio between AuNRs and CHC on HSA detection was investigated for the CHC-AuNR nanoprobe system. The investigated AuNR/CHC ratios were 4/1, 3/1, and 2/1. As shown in Fig. 3, an increase in spectral shift was observed with decreasing AuNR/CHC ratio for all investigated HSA concentrations. The upper limit in concentration for reliable concentration determination was about 10^5 pM, above this concentration the peak shift plateaued and no significant difference could be detected.

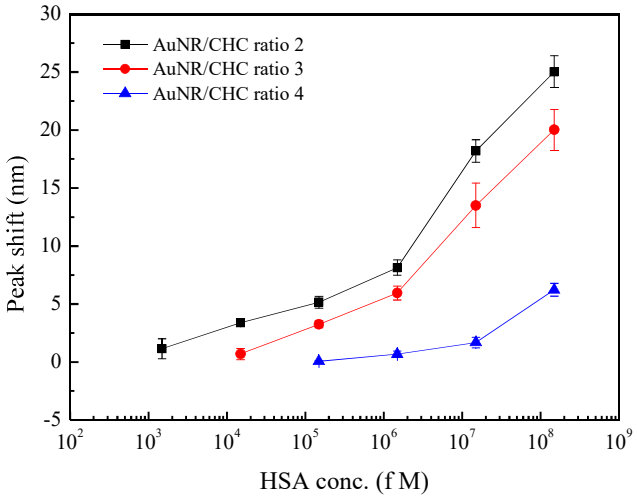

Fig. 3. Peak shift for the nanoprobe system with different AuNR/CHC ratios in response to different HSA concentrations in SU.

The LDL was as low as ~1.50 pM for an AuNR/CHC ratio of 2, which was a 100-fold improvement compared to the LDL for an AuNR/CHC ratio of 4. Furthermore, at this ratio the peak shift in response to HSA concentration was larger than that observed for dispersed AuNRs in previous work.[24] Unfortunately, further reduction of the AuNR/CHC ratio resulted in poor signal-to-noise that prevented reliable determination of the peak shift (data not shown). Thus the CHC-AuNR nanoprobe with an AuNR/CHC ratio of 2 can be considered an optimized version of the nanoprobe for use with readily available and low cost UV-visible spectroscopy, allowing for detection of a HSA concentration as low as 1.5 pM in SU. This LDL is a 10-fold improvement compared to that previously reported for the non-optimized CHC-AuNR nanoprobe system in DI water [24], which is quite remarkable considering the complex biding environment in SU. The pM LDL is also lower than what has been reported in the literature for most HSA sensing systems. Some examples of recently reported approaches and their LDLs are: spectrofluorimetric,

LDL = 62 nM [32]; anti-aggregation of Au nanoparticles, LDL = 1.4 nM [33]; flavone-based fluorescent probe, LDL = 1.4 nM [34]; optical quantum dot-based immunosensor, LDL = 480 pM [35]. A LDL in the attomolar range has recently been reported against IgE proteins for an AuNR-SPR-based sensor [36]. Even if that technology has a lower LDL, it relied on SPR-specific instrumentation, an analysis time in the hours-range and analyses were seemingly conducted in non-complex solutions. In contrast, the CHC-AuNR system holds merit in that it can be used with readily available UV-visible instruments, offers fast analysis time (as further discussed in section 3.3. below) and that the performance was demonstrated in SU. Although speculative, extrapolation of the AuNR/CHC ratio towards lower values, as given in Fig. 4, also suggests that a lower LDL may be possible for the CHC-AuNR nanoprobe by utilization of spectroscopic techniques/instruments that enable acquisition of spectra with higher signal-to-noise at lower AuNR/CHC ratios. For example, the extrapolation indicates that a LDL of 100 fM could be achieved for an AuNR/CHC ratio of 1.2.

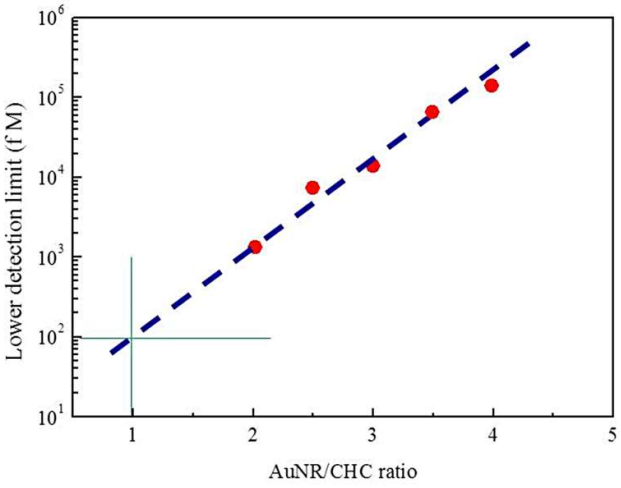

Fig. 4. Lower detection limit for the CHC-AuNR nanoprobe system with different AuNR/CHC ratios. Extrapolation suggests that a lower detection limit of 100 fM may be possible for an AuNR/CHC ratio of 1.2 (indicated by the cross).

3.3. Kinetics of HSA adsorption

The spectral shift is a result from HSA adsorption on the AuNR surface. The kinetics of the deposition will determine the time required to reach equilibrium. This will in turn determine the response time of the biosensor system as equilibrium is needed to reliably determine the concentration of the analyte. Therefore, adsorption kinetics of HSA onto the nanoprobe system with an AuNR/CHC ratio of 2 was investigated by observing the peak shift over time for HSA concentrations in the range 150 pM - 150 nM.

As seen in Fig. 5, the spectral shift reached a plateau in less than 900 seconds for all investigated HSA concentrations, with the equilibrium seemingly being established quicker for lower concentrations. Based on the results it was concluded that an incubation time of 15 minutes was enough to ensure that the peak shift was close to equilibrium for relevant concentrations of HSA. Importantly, this time is short enough to allow for practical use of the nanoprobe system.

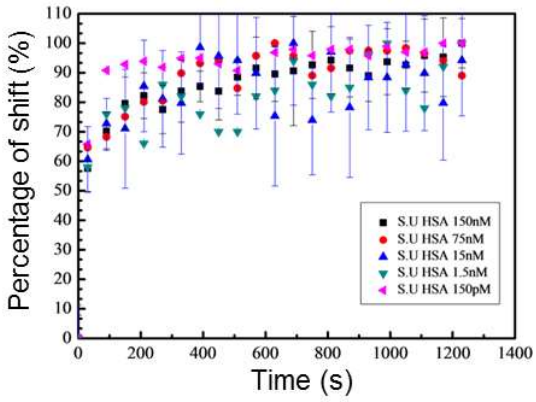

Fig. 5. The relative peak shift over time for the nanoprobe system with an AuNR/CHC ratio of 2 when exposed to SU with different HSA concentrations.

To further understand the concentration dependent adsorption of HSA onto the

nanorods elemental mapping was conducted after exposing the nanoprobe system to SU with 150 pM or 150 nM HSA. As seen in Fig. 6a, sulfur mapping indicated that in 150 pM HSA there was some HSA adsorbed on the AuNR surface with only a very small number of molecules in the surroundings. On the other hand, in 150 nM HSA the AuNR was nearly fully covered with HSA while the surrounding still presented a lower concentration of randomly distributed molecules (Fig. 6b). These results confirm that there was preferential adsorption of HSA onto the AuNRs also in SU. The attractive interactions have previously been attributed to pH-dependent electrostatic interactions in DI water [24] and the mechanism should be the same in SU.

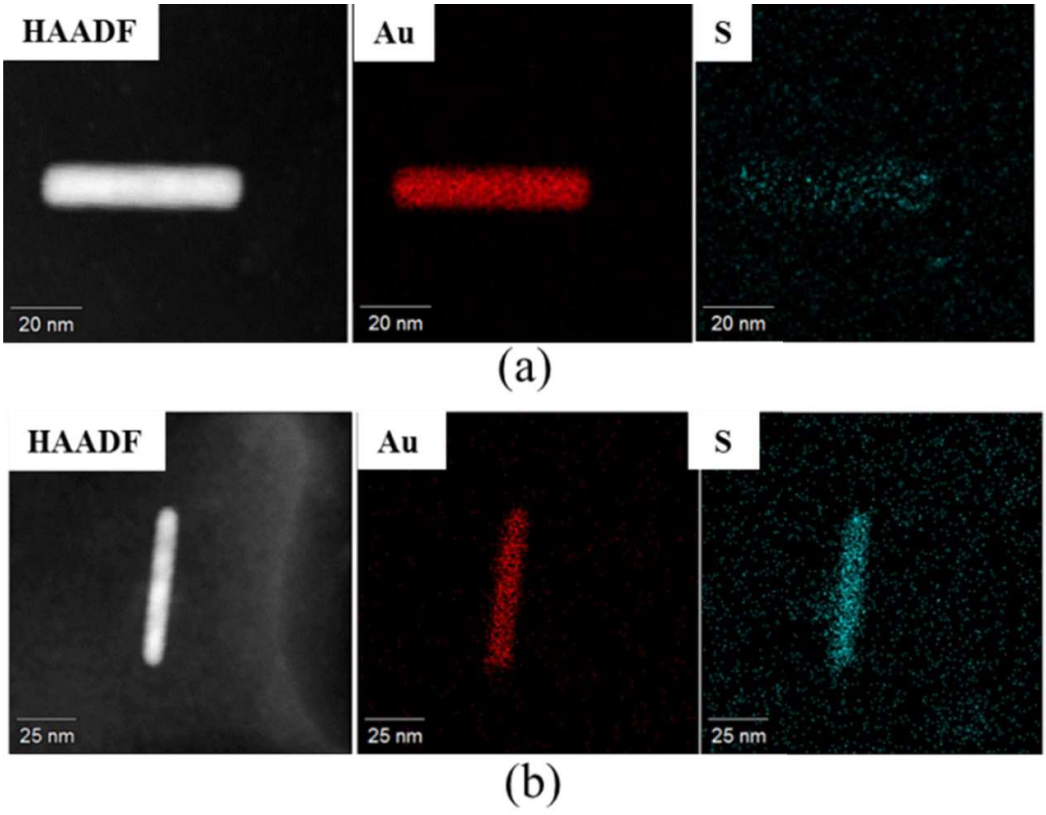

Fig. 6. TEM high angle annular dark field (HAADF) and elemental mapping images of an AuNR in the nanoprobe system after exposure to SU containing (a) 150 pM HSA concentration and (b) 150 nM HSA.

4. Conclusions

The biosensing concept of electrostatic-based, pH-dependent analyte specificity of AuNRs adsorbed on self-assembled CHC nanocarriers was optimized and demonstrated to achieve sensitive detection of HSA in SU. By controlling the ratio between AuNRs and CHC nanocarriers the response and sensitivity (lower detection limit) could be tuned. The results indicated that the lower the AuNR to CHC ratio, the better the response and sensitivity. However, due to limitations from signal-to-noise in the used UV-visible spectroscopic methodology, the lowest ratio that was practically feasible was an estimated 2 AuNRs per CHC nanocarrier, allowing for detection of 1.5 pM HSA in SU, a 100-fold improvement compared with the ratio of 4/1. Furthermore, this LDL was a 10-fold improvement compared to that previously reported for a non-optimized CHC-AuNR system in the less complex environment of DI water. This pM LDL is also lower than what has been reported in recent literature for several HSA-sensing systems [32-35]. The results confirm the potential for using this sensitive nanoprobe in complex environments. It is however recognized that further experiments and optimization, using real urine samples from patients, is required to evaluate the potential of the system to indicate disease from urine tests in a clinical setting. In real samples any peak shift-analyte concentration correlations may be confounded by presence of other organic molecules that also adsorb at a given pH and their inter-individual variations. To circumvent this problem we hypothesize that a multivariate approach may be used to screen for diseases by recording the peak shift at different pH's, in essence generating a pH-peak shift fingerprint characteristic for certain conditions, which could provide extremely powerful if successful. Such investigations will, however, require a large number of participants with clinically

classified conditions and will thus be a subject of future investigations. While more sensitive techniques are available, the nanoprobe system should hold merit in that it is ligand-free and utilizes readily available UV-visible spectroscopy for analysis.

Acknowledgments

We would like to gratefully acknowledge the financial support by the Ministry of Science and Technology under contract number: NSC-100-2622-M-009-002-CC3. We also thank Industrial Technology Research Institute (ITRI) Taiwan, for technical support of this work.

References

[1] W.E. Doering, M.E. Piotti, M.J. Natan, R.G. Freeman, SERS as a Foundation for Nanoscale, Optically Detected Biological Labels, Adv. Mater., 19 (2007) 3100-3108.

[2] R. Elghanian, J.J. Storhoff, R.C. Mucic, R.L. Letsinger, C.A. Mirkin, Selective Colorimetric Detection of Polynucleotides Based on the Distance-Dependent Optical Properties of Gold Nanoparticles, Science, 277 (1997) 1078-1081.

[3] D.J. Maxwell, J.R. Taylor, S. Nie, Self-Assembled Nanoparticle Probes for Recognition and Detection of Biomolecules, J. Am. Chem. Soc., 124 (2002) 9606-9612.

[4] G. Lu, L. Hou, T. Zhang, J. Liu, H. Shen, C. Luo, Q. Gong, Plasmonic Sensing via Photoluminescence of Individual Gold Nanorod, J. Phys. Chem. C, 116 (2012)

25509-25516.

[5] L. Vigderman, B.P. Khanal, E.R. Zubarev, Functional Gold Nanorods: Synthesis, Self-Assembly, and Sensing Applications, Adv. Mater., 24 (2012) 4811-4841.

[6] X. Han, X. Fang, A. Shi, J. Wang, Y. Zhang, An electrochemical DNA biosensor based on gold nanorods decorated graphene oxide sheets for sensing platform, Anal. Biochem., 443 (2013) 117-123.

[7] N.J. Durr, T. Larson, D.K. Smith, B.A. Korgel, K. Sokolov, A. Ben-Yakar, Two-Photon Luminescence Imaging of Cancer Cells Using Molecularly Targeted Gold Nanorods, Nano Lett., 7 (2007) 941-945.

[8] C.J. Murphy, A.M. Gole, S.E. Hunyadi, J.W. Stone, P.N. Sisco, A. Alkilany, B.E. Kinard, P. Hankins, Chemical sensing and imaging with metallic nanorods, Chem. Commun., (2008) 544-557.

[9] J. Qian, L. Jiang, F. Cai, D. Wang, S. He, Fluorescence-surface enhanced Raman scattering co-functionalized gold nanorods as near-infrared probes for purely optical in vivo imaging, Biomaterials, 32 (2011) 1601-1610.

[10] C. Gui, D.-x. Cui, Functionalized Gold Nanorods for Tumor Imaging and Targeted Therapy, Cancer Biology & Medicine, 9 (2012) 221-233.

[11] X. Huang, I.H. El-Sayed, W. Qian, M.A. El-Sayed, Cancer Cells Assemble and Align Gold Nanorods Conjugated to Antibodies to Produce Highly Enhanced, Sharp,

and Polarized Surface Raman Spectra: A Potential Cancer Diagnostic Marker, Nano Lett., 7 (2007) 1591-1597.

[12] S. Park, Y.J. Son, K.W. Leong, H.S. Yoo, Therapeutic nanorods with metallic multi-segments: Thermally inducible encapsulation of doxorubicin for anti-cancer therapy, Nano Today, 7 (2012) 76-84.

[13] J. Wang, G. Zhu, M. You, E. Song, M.I. Shukoor, K. Zhang, M.B. Altman, Y. Chen, Z. Zhu, C.Z. Huang, W. Tan, Assembly of Aptamer Switch Probes and Photosensitizer on Gold Nanorods for Targeted Photothermal and Photodynamic Cancer Therapy, ACS Nano, 6 (2012) 5070-5077.

[14] J. Wang, R. Polsky, D. Xu, Silver-Enhanced Colloidal Gold Electrochemical Stripping Detection of DNA Hybridization, Langmuir, 17 (2001) 5739-5741.

[15] J. Wang, D. Xu, R. Polsky, Magnetically-Induced Solid-State Electrochemical Detection of DNA Hybridization, J. Am. Chem. Soc., 124 (2002) 4208-4209.

[16] H. Hossam, Chemical sensors based on molecularly modified metallic nanoparticles, J. Phys. D: Appl. Phys., 40 (2007) 7173.

[17] B. Baruah, C. Craighead, C. Abolarin, One-Phase Synthesis of Surface Modified Gold Nanoparticles and Generation of SERS Substrate by Seed Growth Method, Langmuir, 28 (2012) 15168-15176.

[18] B. Nikoobakht, M.A. El-Sayed, Surface-Enhanced Raman Scattering Studies on

Aggregated Gold Nanorods†, J.of Phys. Chem. A, 107 (2003) 3372-3378.

[19] M.-C. Daniel, D. Astruc, Gold Nanoparticles: Assembly, Supramolecular Chemistry, Quantum-Size-Related Properties, and Applications toward Biology, Catalysis, and Nanotechnology, Chem. Rev., 104 (2004) 293-346.

[20] F. Caruso, Nanoengineering of Particle Surfaces, Adv. Mater., 13 (2001) 11-22.

[21] R. Ghosh Chaudhuri, S. Paria, Core/Shell Nanoparticles: Classes, Properties, Synthesis Mechanisms, Characterization, and Applications, Chem. Rev., 112 (2012) 2373-2433.

[22] L. He, Y. Liu, J. Liu, Y. Xiong, J. Zheng, Y. Liu, Z. Tang, Core–Shell Noble-Metal@Metal-Organic-Framework Nanoparticles with Highly Selective Sensing Property, Angew. Chem., Int. Ed., 52 (2013) 3741-3745.

[23] K.A. Willets, R.P. Van Duyne, Localized Surface Plasmon Resonance Spectroscopy and Sensing, Annu. Rev. Phys. Chem., 58 (2007) 267-297.

[24] R.-D. Jean, W.-D. Cheng, M.-H. Hsiao, F.-H. Chou, J.-S. Bow, D.-M. Liu, Highly electrostatically-induced detection selectivity and sensitivity for a colloidal biosensor made of chitosan nanoparticle decorated with a few bare-surfaced gold nanorods, Biosens. Bioelectron., 52 (2014) 111-117.

[25] S. Link, M.B. Mohamed, M.A. El-Sayed, Simulation of the Optical Absorption Spectra of Gold Nanorods as a Function of Their Aspect Ratio and the Effect of the

Medium Dielectric Constant, J. Phys Chem. B, 103 (1999) 3073-3077.

[26] K.-S. Lee, M.A. El-Sayed, Gold and Silver Nanoparticles in Sensing and Imaging: Sensitivity of Plasmon Response to Size, Shape, and Metal Composition, J. Phys Chem. B, 110 (2006) 19220-19225.

[27] J. Cao, T. Sun, K.T.V. Grattan, Gold nanorod-based localized surface plasmon resonance biosensors: A review, Sens. Actuators, B, 195 (2014) 332-351.

[28] G.J. Nusz, A.C. Curry, S.M. Marinakos, A. Wax, A. Chilkoti, Rational Selection of Gold Nanorod Geometry for Label-Free Plasmonic Biosensors, ACS Nano, 3 (2009) 795-806.

[29] S.K. Dondapati, T.K. Sau, C. Hrelescu, T.A. Klar, F.D. Stefani, J. Feldmann, Label-free Biosensing Based on Single Gold Nanostars as Plasmonic Transducers, ACS Nano, 4 (2010) 6318-6322.

[30] M.M. Hussain, T.M. Samir, H.M.E. Azzazy, Unmodified gold nanoparticles for direct and rapid detection of Mycobacterium tuberculosis complex, Clin. Biochem., 46 (2013) 633-637.

[31] G.J. Nusz, S.M. Marinakos, A.C. Curry, A. Dahlin, F. Höök, A. Wax, A. Chilkoti, Label-Free Plasmonic Detection of Biomolecular Binding by a Single Gold Nanorod, Anal. Chem., 80 (2008) 984-989.

[32] A.M. Ramezani, J.L. Manzoori, M. Amjadi, A. Jouyban, Spectrofluorimetric

Determination of Human Serum Albumin Using Terbium-Danofloxacin Probe, Sci. World J., 2012 (2012) 9.

[33] Z. Huang, H. Wang, W. Yang, Gold Nanoparticle-Based Facile Detection of Human Serum Albumin and Its Application as an INHIBIT Logic Gate, ACS Appl. Mater. Interfaces, 7 (2015) 8990-8998.

[34] B. Liu, Y. Pang, R. Bouhenni, E. Duah, S. Paruchuri, L. McDonald, A step toward simplified detection of serum albumin on SDS-PAGE using an environment-sensitive flavone sensor, Chem. Commun., 51 (2015) 11060-11063.

[35] M.-C. Tu, Y.-T. Chang, Y.-T. Kang, H.-Y. Chang, P. Chang, T.-R. Yew, A quantum dot-based optical immunosensor for human serum albumin detection, Biosens. Bioelectron., 34 (2012) 286-290.

[36] H.R. Sim, A.W. Wark, H.J. Lee, Attomolar detection of protein biomarkers using biofunctionalized gold nanorods with surface plasmon resonance, Analyst, 135 (2010) 2528-2532.